Analysis and Improvement of a Human Ventricular Cell Model for Investigation of Cardiac Arrhythmias

J Carro[1,2], JF Rodríguez[1], P Laguna[1,2], E Pueyo[1,2]

[1]Instituto de Investigación en Ingeniería de Aragón (I3A), Universidad de Zaragoza, Spain
[2]CIBER de Bioingeniería, Biomateriales y Nanomedicina (CIBER-BBN), Spain

Abstract

The use of experiments for studying cardiac arrhythmias, the effect of drugs, or pathologies on cardiac electrophysiology is very limited. This has made mathematical modeling and simulation of heart's electrical activity a fundamental tool to understand cardiac behavior. In this study several modifications were introduced to a recently proposed human ventricular cell model. Four stimulation protocols were applied to the original and improved models of isolated cell, and a number of cellular arrhythmic risk biomarkers were computed: steady-state action potential (AP) and $[Ca^{2+}]$ transient properties, AP duration (APD) restitution curves, APD adaptation to abrupt changes in heart rate, and intracellular $[Ca^{2+}]$ and $[Na^+]$ rate dependence. Our modifications led to: a) further improved AP triangulation (78.1 ms); b) APD rate adaptation curves characterized by fast and slow time constants within physiological ranges (10.1 s and 105.9 s); c) maximum S1S2 restitution slope in accordance with experimental data ($S_{S1S2} = 1.0$).

1. Introduction

Ventricular arrhythmias can have their origin in diseases, genetic disorders, drug cardiotoxicity, and a number of other causes. Research in this field has identified a number of potential biomarkers of arrhythmic risk related to cellular electrophysiological properties. However, performing experimental and clinical studies involving human hearts to quantify these biomarkers is very difficult. On the other hand, animal hearts used for experimental studies may differ significantly from human hearts. In addition, ventricular cardiac arrhythmias are three-dimensional phenomena whereas experimental observations are still largely constrained to surface recordings. Under this circumstances, mathematical models of myocardial cells and computer simulations of cardiac activity in the human heart can overcome some of these problems.

Recently, a new model has been proposed by Grandi et al. [1] (GR) that improves the response to frequency changes and has a better performance against current blocks with respect to the model proposed by ten Tusscher and Panfilov [2] (TTP06). This article introduces several modifications to the GR model by accounting for recent experimental measurements of potassium currents [3] and the introduction of fast and slow inactivation of L-type calcium current [2]. The performance of the proposed model, herein denoted by CRR, has been tested against the GR and TTP06 models by applying four stimulation protocols and computing twelve cellular arrhythmic risk biomarkers following the methodology proposed in [4]. The results show that the introduced modifications have brought most biomarkers into the physiological range, and considerably improved others with respect to the GR and TTP06 models of AP.

2. Methods

2.1. Biomarkers of arrhythmic risk

Four stimulation protocols have been applied and twelve cellular biomarkers of arrhythmic risk have been computed as in [4]:

Steady-state AP and intracellular $[Ca^{2+}]$ concentration properties. Systolic and diastolic $[Ca^{2+}]_i$ levels under steady-state pacing at frequencies of 0.5 and 1 Hz and APD and AP Triangulation at 1 Hz have been calculated. These biomarkers have been proposed as arrhythmic risk biomarkers in the literature [5–7].

APD restitution (APDR) curves. APDR curves have been obtained using the S1S2 and the dynamic restitution protocols as in [4]. In both cases, the maximum slope, suggested as a risk marker in the literature [8,9], has been computed.

APD rate adaptation to abrupt changes in cycle length (CL). APD rate adaptation dynamics have been proposed as a clinical marker in [10]. Dynamics have been fitted to two exponentials with time constants τ_{fast} and τ_{slow} [11].

Rate dependence of steady-state $[Na^+]_i$ and $[Ca^{2+}]_i$.

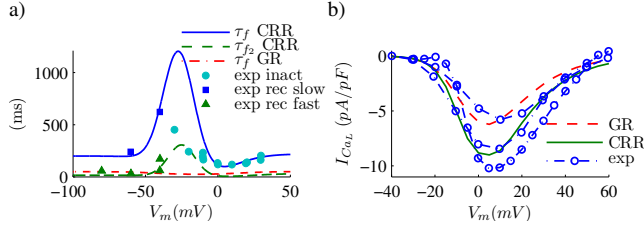Figure 1. $I_{\mathrm{Ca_L}}$ *characteristics in simulations and experiments:* a) Inactivation time constants; b) current density versus voltage. Markers: experimental data.
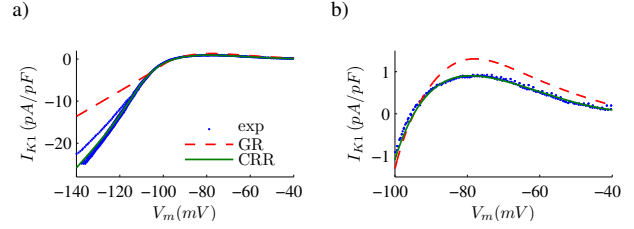

Figure 2. Maximum I_{K1} versus voltage and experimental data. $[K^+]_i = 138\ mM$ and $[K^+]_o = 4\ mM$. Blue dots: experimental data.

The importance of $[Na^+]_i$ and $[Ca^{2+}]_i$ dynamics in arrhythmogenesis has been reported [12, 13]. The systolic values of both concentrations have been measured at different frequencies (0.25, 0.5, 1, 1.5, 2, 2.5 and 3 Hz) and normalized to the level of the minimum frequency. The maximum value has been computed and used as biomarker.

2.2. Modifications of the model

Two ionic currents have been reformulated and some model parameters have been redefined in the GR model:

L-Type Calcium Current ($I_{\mathrm{Ca_L}}$). The voltage-dependent inactivation gate f has been replaced with the product of a fast, f, and a slow, f_2, inactivation gates as in [2]. Based on available experimental data, the value of the opening rate α_{f_2}, associated with f_2, has been modified to:

$$\alpha_{f_2} = 300 \cdot e^{-\frac{(V_m+25)^2}{170}},$$

where V_m denotes the transmembrane potential.

Figure 1a depicts τ_f and τ_{f_2} along with experimental data [2]. The time constant (τ_d) of the activation gate d has been replaced with the description given in [2]. The relative permeabilities of the L-type calcium channels have been adjusted to: $p_{\mathrm{Ca}} = 1.458 \cdot 10^{-4}\ cm/s$, $p_{\mathrm{K}} = 7.290 \cdot 10^{-8}\ cm/s$, $p_{\mathrm{Na}} = 4.050 \cdot 10^{-9}\ cm/s$.

This new definition of $I_{\mathrm{Ca_L}}$ is compared against experimental data and the original definition of the GR model in Figure 1b. Experimental data is from [14–16].

Inward Rectifier K Current (I_{K1}). This current has been re-adjusted based on experimental data from [3]. The re-adjusted current is formulated as follows:

$$V_{\mathrm{E}_k} = V_m - E_k$$

$$a_{\mathrm{K1}} = \frac{4.094}{1.0 + e^{0.1217 \cdot \left(V_{\mathrm{E}_k} - 49.934\right)}}$$

$$b_{\mathrm{K1}} = \frac{15.720 \cdot e^{0.0674 \cdot \left(V_{\mathrm{E}_k} - 3.257\right)} + e^{0.0618 \cdot \left(V_{\mathrm{E}_k} - 594.31\right)}}{1.0 + e^{-0.1629 \cdot \left(V_{\mathrm{E}_k} + 14.207\right)}}$$

$$K1_{ss} = \frac{a_{\mathrm{K1}}}{a_{\mathrm{K1}} + b_{\mathrm{K1}}}$$

$$I_{\mathrm{K1}} = 0.5715 \cdot \sqrt{\frac{[K^+]_o}{5.4}} \cdot K1_{ss} \cdot V_{\mathrm{E}_k}$$

where $[K^+]_o$ denotes the extracellular K^+ concentration, and E_K is the K^+ reversal potential. Figure 2 shows the modified I_{K1} compared against the experimental data from [3] and I_{K1} from the GR model. Note that Figure 2b is a zoom from Figure 2a.

$I_{\mathrm{Na,K}}$: *Na/K Pump Current.* Maximal $I_{\mathrm{Na,K}}$ conductance has been reduced by 45%.

$[K^+]_i$ *and* G_{Na}. A more physiological value of $[K^+]_i$ (138 mM) has been used in the model. In this regard, in order to get physiological values for the maximal upstroke velocity, dV/dt, the maximum conductance of the sodium current, G_{Na}, has been reduced to 18.86 $mS/\mu F$.

2.3. Blocking Currents

We have also studied the behavior of the model under total and partial block of potassium currents, comparing the results against those reported in [17]:

I_{Ks}: To simulate the effect of 1 μM of HMR-1556, I_{Ks} has been completely blocked.

I_{Kr}: To simulate the effect of 50 nM of dofetilide, I_{Kr} has been completely blocked.

I_{K1}: To simulate the effect of 10 μM of $BaCl_2$, I_{K1} has been blocked at 50%.

2.4. Numerical implementation and simulation

Model differential equations were implemented in Fortran. Cells were stimulated with square transmembrane current pulses twice the diastolic threshold at CL = 1000 ms and 1-ms duration. Forward Euler integration with a time step $\Delta t = 0.002\ ms$ was used to integrate the system of differential equations governing the cellular electrical behavior. The Rush and Larsen integration scheme was used to integrate the Hodgkin-Huxley type equations for the gating variables of the various time-dependent currents.

Biomarker	TTP06	GR	CRR	Physiolo.
APD_{90}	301.2	285.0	306.1	271-366
Triangulation	28.4	51.5	78.1	44-112
Sys $[Ca^{2+}]_i$ 1 Hz	0.886	0.383	0.602	1.59-2.01
Sys $[Ca^{2+}]_i$ 0.5 Hz	0.199	0.345	0.522	0.71-1.68
Dia $[Ca^{2+}]_i$ 1 HZ	0.104	0.089	0.097	0.20-0.33
Dia $[Ca^{2+}]_i$ 0.5 Hz	0.068	0.085	0.091	0.14-0.32
$S_{max_{S1S2}}$	1.3	0.2	1.0	0.79-4.25
$S_{max_{DYN}}$	1.0	1.1	0.9	—
τ_{fast}	13.3	—	10.1	—
τ_{slow}	124.8	56.3	105.9	70-110
Max. sys. $[Ca^{2+}]_i$	1157	178	147	130-170
Max. sys. $[Na^+]_i$	217	132	134	145

Table 1. Biomarkers of arrhythmic risk for the TTP06, GR and CRR human models. Green color indicates within physiological range. Blue color indicates out of physiological range but better than previous models. Red color indicates out of physiological range.

3. Results

3.1. Biomarkers of arrhythmic risk

Table 1 shows the computed biomarkers for the modified model, CRR. Results are compared against those obtained with previous models (TTP06 and GR) and against a variety of physiological data described in [4].

These results indicate that the GR model performs better than the TTP06 model, with respect to the following biomarkers: triangulation, systolic and diastolic $[Ca^{2+}]_i$ at 0.5 Hz and rate dependence of steady-state $[Na^+]_i$ and $[Ca^{2+}]_i$. However, according to other analyzed biomarkers, the GR model renders worse results than the TTP06 model. Particularly, in [18] two phases of APD rate adaptation curve were reported: a first phase with a rapid time constant and a second phase with a slower time constant. The GR model does not present this first phase. Also, the S1S2 restitution curves of the TTP06 model (Figure 3c) are in better agreement with experimental data.

For the CRR model, most of the twelve analyzed biomarkers are within the physiological range or otherwise closer to the physiological range as compared to GR and TTP06 models, except for systolic and diastolic $[Ca^{2+}]_i$ levels at 0.5 Hz where TTP06 outperforms CRR.

3.2. Blocking Currents

Table 2 summarizes the effect of current block on the different models. Results are given as percentage of variation of the APD value in control conditions. In those cases where more than one current is blocked, the variation refers to the APD obtained when the first current is
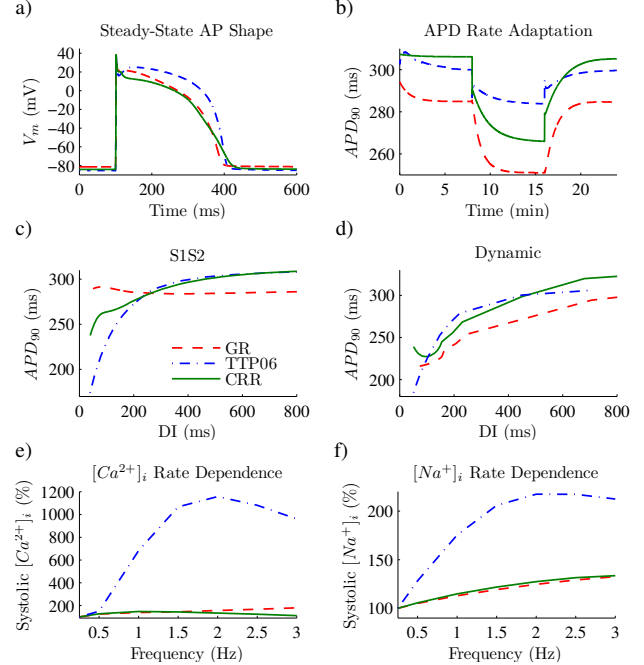

Figure 3. Biomarkers of arrhythmic risk from TTP06, GR and CRR models: a) AP for CL = 1000 ms; b) APD rate adaptation to abrupt changes in CL (From 1000 ms to 600 ms); c) S1S2 restitution protocol curve; d) Dynamic restitution protocol curve; e) rate dependence of steady-state $[Na^+]_i$; f) rate dependence of steady-state $[Ca^{2+}]_i$

blocked. Experimental values have been taken from [17].

4. Discussion and conclusions

This study introduces several modifications to the GR model by accounting for recent experimental measurements of potassium currents, and by reformulating the L-type calcium current so as to introduce fast and slow voltage-dependent inactivation. All the modifications have been made with the aim of maintaining the advantages that the GR model presents over previous models while improving the performance on other electrophysiological aspects.

For the proposed CRR model, the introduction of fast and slow I_{Ca_L} inactivation has led to a more physiological rate adaptation response as compared to the original GR model. The other modifications have rendered most biomarkers to be within the physiological range or otherwise closer to the physiological range as compared to the GR and TTP06 models, except for systolic and diastolic $[Ca^{2+}]_i$ levels at 0.5 Hz where TTP06 outperforms CRR. These modifications, however, have altered the behavior of the model against current blocks minimally.

The results of the analysis conducted in this study points out the importance that calcium dynamics have over differ-

Current	Ref.	TT	GR	CRR	Exper.
I_{Kr} 0%	Control	74.9	0.7	0.6	< 2.8
I_{Kr} 0%	Control	15.9	18.6	14.1	44±4
I_{Ks} 0%	I_{Kr} B.	—	1.4	0.8	9
I_{Kr} 0%					
I_{K1} 50%	Control	3.6	11.5	14.6	4.8±1.5
I_{Kr} 0%	I_{Kr} B.	8.9	15.6	21.1	33
I_{K1} 50%					

Table 2. Percentages of variation in the APD caused by blocking different currents. Green color indicates within physiological range. Blue color indicates out of physiological range but better than previous models. Red color indicate out of physiological range.

ent biomarkers. This suggests the need for continuing with the development of more reliable calcium dynamic models that allow improving the performance of whole cell AP models.

Further developments of the proposed model will include conducting a sensitivity analysis of the studied biomarkers to changes in model parameters as proposed in [4], as well as testing the performance of the model under pathological conditions such as hyperkalemia.

Acknowledgements

References

[1] Grandi E, Pasqualini FS, Bers DM. A novel computational model of the human ventricular action potential and ca transient. J Mol Cell Cardiol 2010;48:112 – 121.

[2] ten Tusscher K, Panfilov A. Alternans and spiral breakup in a human ventricular tissue model. Am J Physiol Heart Circ Physiol 2006;291:H1088–H1100.

[3] Fink M, Noble D, Virag L, Varro A, Giles WR. Contributions of herg k+ current to repolarization of the human ventricular action potential. Progress in Biophysics and Molecular Biology 2008;96:357 – 376. ISSN 0079-6107.

[4] Romero L, Pueyo E, Fink M, Rodríguez B. Impact of ionic current variability on human ventricular cellular electrophysiology. Am J Physiol Heart Circ Physiol 2009; 297:H1436–1445.

[5] Bers DM, Despa S. Cardiac myocytes ca2+ and na+ regulation in normal and failing hearts. J Pharm Sci 2006; 100:315–322.

[6] Hondeghem L, Carlsson L, Duker G. Instability and triangulation of the action potential preict serious proarrhythmia, but action potential duration prolongation is antiarrhythmic. Circ 2001;103:2004–2013.

[7] Volders P, Vos M, Szabo B, Sipido K, de Groot S, Gorgels A, Wellens H, Lazzara R. Progress in the understanding of cardiac early afterdepolarizations and torsades de pointes: time to revise current concepts. Cardiovasc Res 2000; 46:376–392.

[8] Nolasco J, Dahlen R. A graphic method for the study of alternation in cardiac action potentials. J Appl Physiol 1968; 25:191–196.

[9] Weiss J, Karma A, Shiferaw U, Chen P, Garfinkel A, Qu Z. From pulses to pulseless: the saga of cardiac alternans. Circ Res 2006;98:1244–1253.

[10] Pueyo E, Smetana P, Caminal P, de Luna A, Malik M, Laguna P. Characterization of qt interval adaptation to rr interval changes and its use as a risk-stratifier of arrhythmic mortality in amiodarone-treated survivors of acute myocardial infarction. IEEE Trans Biomed Eng 2004;51:1511–1520.

[11] Pueyo E, Husti Z, Hornyik T, Baczkó I, Laguna P, Varró A, Rodríguez B. Mechanisms of ventricular rate adaptation as a predictor of arrhythmic risk. Am J Physiol Heart Circ Physiol 2010;298:H1577–H1587.

[12] Levi A, Dalton G, Hancox J, Mitcheson J, Issberner J, Bates J, Evans S, Howarth F, Hobai I, Jones J. Role of intracellular sodium overload in the genesis of cardiac arrhythmias. J Cardiovasc Electrophysiol 1997;8:700–721.

[13] Murphy E, Eisner D. Regulation of intracellular and mitochondiral sodium in health and disease. Circ Res 2009; 104:292–303.

[14] Pelzmann B, Schaffer P, Bernhart E, Lang P, Machler H, Rigler B, Koidl B. L-type calcium current in human ventricular myocytes at a physiological temperature from children with tetralogy of fallot. Cardiovasc Res 1998;38:424–432.

[15] Li GR, Yang B, Feng J, Bosch RF, Carrier M, Nattel S. Transmembrane ica contributes to rate-dependent changes of action potentials in human ventricular myocytes. Am J Physiol Heart Circ Physiol 1999;276:H98–106.

[16] Magyar J, Iost N, Körtvély Á, Bányász T, Virág L, Szigligeti P, Varró A, Opincariu M, Szécsi J, Papp JG, Nánási PP. Effects of endothelin-1 on calcium and potassium currents in undiseased human ventricular myocytes. Pflugers Arch 2000;441:144–149.

[17] Jost N, Varro A, Szuts V, Kovacs PP, Seprényi G, Biliczki P, Lengyel C, Prorok J, Bitay M, Ördög B, Szabad J, Varga-Orvos Z, Puskas L, Cotella D, Papp JG, Virag L, Nattel S. Molecular basis of repolarization reserve differences between dogs and man. Circ 2008;118 Suppl-2:S342 (abstract).

[18] Franz MR, Swerdlow CD, Liem LB, Schaefer J. Cycle length dependence of human action potential duration in vivo. Am Clin Inves 1988;82:972–979.

Address for correspondence:

Jesús Carro Fernández
Campus Río Ebro. Edificio I+D+i. Laboratorio 5.1.02
C/ Mariano Esquilor s/n. CP: 50.018 - Zaragoza, SPAIN.
jcarro@unizar.es